Yamato *et al. Int J Concr Struct Mater* (2020) 14:16
https://doi.org/10.1186/s40069-020-0391-7

International Journal of Concrete Structures and Materials

RESEARCH Open Access

Resistance Properties to Chloride Ingress of Standard-Cured Concrete Made with an Admixture Incorporating Rich SiO_2 and Al_2O_3

Koichiro Yamato[1], Akira Sasaki[1], Takayasu Ito[1] and Isamu Yoshitake[2*]

Abstract

In regions where the concrete structures are exposed to a salty environment, the concrete requires high resistance to chloride-ion penetration. To achieve higher resistance against chloride ingress, a pozzolanic admixture incorporating a high volume of SiO_2 and Al_2O_3 has been developed. The admixture is a fine mineral powder with a specific surface area of 13,000 m^2/kg or higher. It is typically mixed with the concrete at a cement replacement level of 5–13 mass% (20–40 kg/m^3). To demonstrate the applicability of the admixture to general ready-mix concretes, this study examined the fundamental properties of concrete cured under standard conditions regarding resistance against chloride ingress. Chloride immersion tests revealed high resistance against penetration of concrete produced with the admixture. Pore-size distribution analysis confirmed that the volume of pores less than 0.01 μm diameter increased whereas a decrease of large pores occurred (0.1 μm diameter or larger). The major contributor to the high resistance was found to be the immobilization of penetrating chloride ions by the formation of Friedel's salt.

Keywords: admixture, concrete, chloride attack resistance, pore size distribution, Friedel's salt

1 Introduction

Reinforced concrete structures in coastal and snowy regions are generally subjected to chloride attacks and steel corrosion often occurs due to the penetration of chloride ions (Vaysburd and Emmons 2004; Raupach 2015). To reduce future maintenance costs, concretes are required to have a high resistance to chloride ingress (Ministry of Land, Infrastructure and Transport 2015). Such concretes would have a denser structure and achieve excellent durability in various environments.

Mineral admixtures such as fine blast furnace slag powder and fly ash have been used to improve durability of concrete (Juenger and Siddique 2015; Hossain et al. 2016). Celik et al. (2015) reported on physical properties of concrete mixed with fly ash (cement-replacement ratios of 30 and 60%) and limestone powder (cement-replacement ratio of 15 to 25%). In addition, Celik et al. (2014) reported the relevant properties of concrete that incorporated 15% limestone powder and 30% natural volcanic pozzolan by mass of cement. Their investigations confirmed that concretes incorporating these powder materials significantly improved resistance against chloride-penetration. However, it was concerning that the compressive strength of concrete at an early age was significantly lower.

A number of investigations have dealt with the improvement of the early-age strength of concrete incorporating large amounts of admixtures. Meddah et al. (2014) reported on relevant properties of concrete with either 30% blast furnace slag fine powder, 20% fly ash, or

*Correspondence: yositake@yamaguchi-u.ac.jp
[2] Department of Civil and Environmental Engineering, Yamaguchi University, 2-16-1 Tokiwadai, Ube, Yamaguchi 755-8611, Japan
Full list of author information is available at the end of the article
Journal information: ISSN 1976-0485 / eISSN 2234-1315

5% silica fume. Another aim of the use of such by-products as an alternative cementitious material is to mitigate environmental impact.

However, when using large amounts of such by-products for the conservation of the environment, additional storage facilities, such as silos, are required.

Madani et al. (2014) focused on concrete incorporating small amounts of admixture to improve early-age strength and chloride-penetration resistance. They examined the chloride-penetration resistance and compressive strength of concrete incorporating several percentages of nanosilica and silica fume. It is worth noting that the admixture used in this study effectively increased the compressive strength at an early age, even for small additions of the admixture. The manufacturing efficiency of the very fine powdered material is a concern.

The authors of this paper have developed an alternative cementitious admixture to improve resistance to chloride ingress of concrete (Ishida et al. 2015). The standard mixture volume of this admixture is in the range of 5–13 mass% (20–40 kg/m^3), therefore it can be added manually at a batching plant. The admixture can also be used as an alternative binder for Portland cement in addition to other general admixtures, such as fly ash. Use of the admixture may be suitable for precast concrete production factories with limited storage facilities. The admixture is a fine pozzolanic mineral powder with a Brunauer–Emmett–Teller (BET) specific surface area of 13,000 m^2/kg or higher and therefore it can also improve strength development of concrete at an early age.

Mechanical properties and durability of steam-cured concrete mixed with the admixture were examined in our previous investigation (Yamato et al. 2017). The admixture is also useful in general ready-mix concrete plants. To confirm applicability of the admixture for general purposes of ready-mix concrete, the present study examined mechanical properties and durability of standard-cured concrete incorporating this admixture. In addition, the study investigated the chloride resistance mechanism of concrete incorporating the admixture.

Resistance to chloride penetration may be due to (1) densification of hardened cement and (2) chloride-ion adsorption by hydrates (Ishida et al. 2007; Lia et al. 2015). Madani et al. (2014) and Ahmed et al. (2008) reported that hardened cement was densified by the microfiller effect and pozzolanic reaction. To confirm the densification effect (1), pore-size distribution and pore structures were examined using mercury intrusion porosimetry (MIP) measurement system (Elrahman and Hillemeier 2014; Fan et al. 2014). It is well known that chloride ions are chemically bound in Friedel's salt (Lia et al. 2015; Neville 2012). Previous investigations showed that chloride ions were physically and/or electrically adsorbed on the C–S–H surface (Lia et al. 2015; Yoshida et al. 2002). To examine the chloride-ion adsorption effect (2), the study investigated the hydration products, such as Friedel's salt, in cement paste immersed in 3% NaCl solution. The hydrated products were examined using X-ray diffraction (XRD) (Shi et al. 2017; Heisig et al. 2016). In addition, Rietveld analysis was performed to quantify the amount of Friedel's salt and to examine chemical binding of chloride ions in hydrated cement (Shi et al. 2017; Schepper et al. 2014). The amount of bound chloride-ions concentration was estimated by subtracting the amount of free chloride from the total amount of chloride present in the cement paste (Lia et al. 2015).

This paper presents the properties of the developed admixture and describes the mechanism behind the improved resistance to chloride penetration when the admixture is mixed in concrete.

2 Materials and Mixture Proportions of Concrete

2.1 Materials

The developed admixture (CG) is a pozzolanic mineral powder incorporating SiO_2 and Al_2O_3, and it has a Brunauer–Emmett–Teller (BET) specific surface area of 13,000 m^2/kg or higher. Ordinary Portland cement (OPC) (Japan Industrial Standard, JIS A 6207 2011b) and blast furnace cement of type B (BB) (Japan Industrial Standard, JIS A 6204 2011a) were used in the experimental study. These cements have similar properties to EN 197-1, CEM I or CEM III according to EN 197-1 (European standards 2011). In addition, silica fume (SF) was used as a reference admixture for comparison (Japan Industrial Standard, JIS A 6207 2011b). Fundamental properties of the cementitious materials are listed in Table 1. It is remarkable that the admixture (CG) has a significant higher Al_2O_3 than silica fume (SF) while both consist of high SiO_2. Aggregates and chemical admixture as listed in Table 2 were used for the concrete tested in this study (Japan Industrial Standard, JIS A 6204 2011a; ASTM International, ASTM C 494 2004a).

2.2 Mixture Proportions

Mixture proportions are summarized in Table 3. The water cementitious material ratios (***w/cm***) were designed in the range of 0.45 to 0.55 by mass to simulate a general-purpose concrete mixture in ready-mix concrete of Japan. The admixture (CG) was mixed with the fresh concrete as an alternative cementitious material by mass of cement (5–13%). For the comparison, silica fume (SF) was used with a cement-replacement ratio of 13% by mass. The replacement ratio was determined to minimize the diffusion coefficient of chloride ion by referring to the previous research (Farahani et al. 2015). The volume ratio of sea sand (S1) to crushed sand (S2) was

Table 1 Properties of cementitious materials.

Material	Density (kg/m^3)	Fineness (m^2/kg)	CaO (%)	SiO_2 (%)	Al_2O_3 (%)	Na_2O (%)	K_2O (%)	Cl^- (%)
Ordinary portland cement (OPC) (JIS R 5210, 2009a) (EN 197-1, CEM I 52.5)	3160	328[a]	64.6	20.5	5.67	0.17	0.40	0.015
Blast-furnace slag cement (BB) (JIS R 5211, 2009b) (EN 197-1, CEM III/B 52.5)	3040	372[a]	54.2	25.5	9.55	0.19	0.35	0.011
Developed admixture (CG)	2360	13300[b]	–	71.2	23.3	0.27	0.27	0.029
Silica fume (SF)	2240	16900[b]	–	94.0	0.26	0.21	0.28	0.014

[a] Blain fineness.

[b] BET fineness.

Table 2 Properties of aggregates and chemical admixture.

Fine aggregate	Sea sand (S1) Density 2570 kg/m^3, absorption 1.66%, F.M. 2.97 Chloride ion concentration 0.002%
	Crushed sand (S2) Density 2680 kg/m^3, absorption 2.52%, F.M. 2.71
Coarse aggregate	Crushed stone (G), maximum size 20 mm, density 2700 kg/m^3, absorption 0.65%, F.M. 6.77
Chemical admixture	High-range water-reducing agent (HRWRA) (Lignin sulfonate, oxy-carboxylate and polycarboxylic acid-based compound)
	Air entraining agent (AEA) (Alkyl ether-based) (JIS A 6204), (ASTM C 494)

0.5:0.5. The chloride in the sea sand (S1) was negligible because the chloride ion concentration was 0.002%. The unit weight of coarse aggregate was 1050 kg/m^3, which is constant in all mixtures. The designed concrete slump was 80 ± 25 mm, and the air content of the concrete was 4.5 ± 1.5%. The fresh properties of the tested concrete are also listed in Table 3.

2.3 Mixing and Curing Methods

Cementitious materials and aggregates were dry-mixed in a revolving-paddle mixer (max. 0.055 m^3) for 30 s. Thereafter, water with chemical admixture was added to the dry-mixed materials and the concrete was mixed for 120 s. The mixing procedure was decided by referring to previous studies such as an investigation that examined the strength and durability of various cement concretes (Amoudi et al. 2009).

All cylindrical concrete specimens were stored in a curing room (temperature of 20 ± 2 °C and relative humidity of 65 ± 5%) for 24 h. After demolding at an age of 24 h, the specimens were cured in a water tank at 20 ± 2 °C.

3 Test Programs

3.1 Compressive Strength Test

Three concrete cylinders (100 mm diameter × 200 mm height) for each composition were used in the compressive strength test. The compressive strength test was performed at ages of 7, 14 and 28 days in accordance with the Japanese industrial standard (Japanese industrial standard, JIS A 1108 2006) that is equivalent to

Table 3 Mixture proportions and fresh properties of concrete.

Mix. ID[a]	*w/cm*	*Ad/cm* (%)	*s/a*[b] (%)	Unit weight (kg/m^3)						AWA (*cm* × %)	Slump (mm)	Air (%)
				w	*cm*		S1	S2	G			
					C	*Ad*						
OPC (0.45)	0.45	0	41.8	168	373	0	360	372	1050	0.50	90	4.8
OPC-CG 5% (0.45)		5	41.6		353	20	357	370		0.65	100	4.4
OPC-CG 11% (0.45)		11	41.4		333	40	354	367		0.80	85	4.6
OPC (0.55)	0.55	0	43.7		305	0	388	404		0.40	95	4.6
OPC-CG 7% (0.55)		7	43.5		285	20	385	401		0.55	105	4.6
OPC-CG 13% (0.55)		13	43.3		265	40	382	398		0.65	100	5.2
OPC-SF 13% (0.55)		13	43.1		265	40	380	394		1.00	80	4.7
BB (0.55)		0	43.4		305	0	383	399		0.45	105	5.0

[a] Cement—admixture—content (***w/cm***).

[b] Sand-to-aggregate volume ratio.

ISO 1920-4 (The International Organization for Standardization 2005).

3.2 Chloride Migration Test

Chloride migration tests were conducted in accordance with the Japan Society of Civil Engineers standard (JSCE-G571: Test method for effective diffusion coefficient of chloride ion in concrete by migration) (Japan Society of Civil Engineers 2013; Hisada et al. 1999). In this test, the pore solution of concrete is subjected to an electric field, in which negatively charged chloride ions are electrically attracted to the anode under an externally applied voltage. The chloride ion migration flux—the amount of chloride ion per unit area and unit time—can be estimated from the amount of chloride ions transported to the anode. The effective diffusion coefficient can be calculated from the steady-state condition of this migration.

Figure 1 shows the schematics of the chloride ion migration test for concrete. Concrete disks (100 mm dia. × 50 mm thick) were made by cutting cylindrical specimens (100 mm diameter × 200 mm height) at an age of 28 days. The sliced disk was placed into the migration cell. Three disk specimens for each composition were tested in accordance with JSCE-G571. Solutions in the cell were aqueous NaCl (0.5 mol/L) as the catholyte and NaOH (0.3 mol/L) as the anolyte. The volume of each solution was 1000 cm^3 (1 L). A stainless-steel plate was used as the cathode and a titanium plate for the anode. The study examined the amount of chloride ions transferred from cathode to anode under a constant direct voltage of 15 V. It is noted that the chloride concentration in the catholyte was maintained constant at 0.5 mol/L during the test.

During the migration test, the chloride-ion concentration in the anolyte increased. The ionic flux J_{Cl} (mol/$cm^2 s^{-1}$) is proportional to $\Delta C/\Delta t$ and can be calculated using Eq. (1). The effective diffusion coefficient D_e was calculated by employing Eq. 2 (Japan Society of Civil Engineers 2013; Wattanachai et al. 2009).

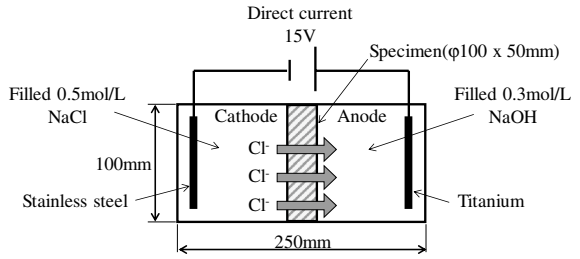

Fig. 1 Test method for ingress of chloride ions in concrete by migration.

$$J_{Cl} = \frac{V_{II}}{A} \cdot \frac{\Delta C}{\Delta t}, \tag{1}$$

where $\boldsymbol{J_{Cl}}$ is the chloride ionic flux in steady state (mol/cm^2 s^{-1}), $\boldsymbol{V_{II}}$ is the amount of solution in anode side cell (cm^3) and $\boldsymbol{A}$ is the cross-sectional area of the concrete specimen (cm^2). $\boldsymbol{\Delta C/\Delta t}$ presents the rate of ionic transfer (mol/L s^{-1}), which means the change with time of the chloride concentration in the anolyte.

$$D_e = \frac{J_{Cl} \cdot R \cdot T \cdot L}{|Z_{cl}| \cdot F \cdot C_{Cl} \cdot (\Delta E - \Delta E_c)} \times 100, \tag{2}$$

where $\boldsymbol{D_e}$ is the effective diffusion coefficient of chloride ion (cm^2/s); $\boldsymbol{R}$ is the gas constant (8.31 J/mol K^{-1}); $\boldsymbol{T}$ is the absolute temperature (K); $\boldsymbol{L}$ is the specimen length (mm); $\boldsymbol{Z_{Cl}}$ is the charge of chloride ion (Cl = − 1); $\boldsymbol{F}$ indicates Faraday's constant (96,500 C/mol); $\boldsymbol{C_{Cl}}$ shows the measured chloride ion concentration on the cathode side (mol/L), and $(\boldsymbol{\Delta E - \Delta E_c})$ presents the electrical potential difference between specimen surfaces (V). The value of $(\boldsymbol{\Delta E - \Delta E_c})$ is obtained from the polarization of both the anode and the cathode.

3.3 Chloride Immersion Test for Concrete

The chloride immersion test was conducted in accordance with the Japan Society of Civil Engineers standard (JSCE-G572: Test method for apparent diffusion coefficient of chloride ion in concrete by submersion in salt water) (Japan Society of Civil Engineers 2013), which is almost the same as that defined by ASTM C 1556 (ASTM International 2004b). A 150-mm-thick cylinder was produced by cutting 25 mm from both ends of a cylindrical specimen (100 mm dia. × 200 mm long) at an age of 28 days. The bottom and side surfaces of the cut cylinders were sealed with epoxy resin to prevent chloride penetration. Thereupon, the sealed cylinders were immersed in a 10% NaCl solution for 91 days. Following this immersion period, the cylinders were sliced into 10-mm-thick disks from the top surface and the chloride concentrations were examined to quantify the chloride distribution. The chloride concentration at each depth was determined in accordance with the Japanese standard (JIS A 1154: Methods of test for chloride ion content in hardened concrete) (Japan Industrial Standard 2012). Pulverized concrete (10 g) and 19% nitric acid solution (70 mL) were stirred for 30 min in a container. The mixed materials were boiled for 5 min to extract the chloride ions and then cooled to room temperature. The mixture was separated by suction filtration into the concrete residue and filtrate. The filtrate was potentiometrically titrated

with silver nitrate using potentiometry and the chloride-ion concentration was calculated based on the amount of titrant consumed. The chloride diffusion coefficient, derived from the immersion test, was determined by curve-fitting the measured chloride profile to Fick's second law, as given in Eq. 3 (Crank 1975, Sabet et al. 2013):

$$C(x,t) - Ci = C_{a0}\left[1 - erf\left(\frac{0.1x}{2\sqrt{D_{ap}t}}\right)\right], \quad (3)$$

where $\boldsymbol{x}$ is the depth (cm), $\boldsymbol{t}$ is the immersion time (s) and $\boldsymbol{C}(\boldsymbol{x}, \boldsymbol{t})$ presents the total chloride content (kg/m^3). $\boldsymbol{C_i}$ is the initial total chloride content (kg/m^3), $\boldsymbol{Ca_0}$ is the total chloride content at the concrete surface (kg/m^3), and $\boldsymbol{D_{ap}}$ is the apparent chloride diffusion coefficient (cm^2/s).

3.4 Pore-Size Distribution

The study examined pore-size distribution and evaluated the pore structure to confirm the densification of hardened cement. Pore size distribution and pore volume in the concrete at an age of 56 days were observed with a Micrometrics Autopore IV 9500 mercury intrusion porosimeter. The tested concretes were crushed to 2.5–5.0 mm and freeze-dried. The pressure of the porosimetry equipment ranged from 0.006 to 412 MPa. Assumed as a cylinder shape pore, Eq. 4 was used to calculate pore-size distribution.

$$\boldsymbol{D} = -(1/\boldsymbol{P})\, 4\boldsymbol{\gamma} \cos\boldsymbol{\theta}, \quad (4)$$

where $\boldsymbol{D}$ is a diameter of pore, P is the pressure, γ is the surface-tension of mercury (485 dyn/cm), and $\boldsymbol{\theta}$ is the contact angle (140°).

3.5 Chloride Immersion Test of Cement Paste

3.5.1 Outline

Chloride ions are chemically incorporated or adsorbed as Friedel's salt ($3CaO{\cdot}Al_2O_3{\cdot}CaCl_2{\cdot}10H_2O$) in case of relatively large amounts of C_3A or Al_2O_3 in cementitious material. In addition, chloride ions are physically or electrically adsorbed onto C–S–H (Lia et al. 2015; Yoshida et al. 2002). However, direct measurement of the amount of adsorbed chloride ion is difficult. To confirm the phenomenon of chemically bound chloride ions, the study examined the hydration products of chloride-immersed cement paste immersed in a chloride solution, such as Friedel's salt, and the amount of bound chloride ions.

The investigation used three bar specimens (40 mm × 40 mm × 160 mm) made with cement paste of $\boldsymbol{w/cm} = 0.50$. The study prepared three mixtures of cement pastes ($\boldsymbol{w/cm} = 0.5$) for 0, 6% and 12% of the admixture CG. All specimens were immediately sealed with a polyethylene film and thereupon cured in a laboratory at a room temperature of 20 ± 2 °C. The specimens were not stored in a water tank to avoid elution of the chemical ingredients. At an age of 28 days, the specimens were crushed to 2.5–5.0 mm and the particles were immersed in a 3% NaCl solution. The amount of bound chloride ions was examined based on a Japanese standard test and the bound water was quantified using differential thermogravimetric analysis (DTA). To examine the hydrated products, XRD analysis was performed after immersion periods of 0, 28, and 91 days. Each test method is described in the following sections.

3.5.2 Bound Chloride-Ion Content

The chloride ions bound in the cement paste were quantified by subtracting the free chloride-ion content from the total chloride-ion content. The cement paste samples were prepared by freeze-drying and pulverized using a vibration mill. The total chloride-ion content was examined by extracting these from the cement paste using nitric acid, in accordance with the Japanese standard (Japan Industrial Standard, JIS A 1154 2012). Pulverized cement paste (10 g) and nitric acid solution (19%) (70 mL) were stirred for 30 min in a container and then boiled for 5 min to extract the chloride ions. After cooling, the mixture was separated by suction filtration into the cement paste residue and the filtrate. The filtrate was potentiometrically titrated against silver nitrate using potentiometry and the chloride-ion concentration was calculated based on the consumed titrant.

The free chloride ions, water-soluble chloride, were quantified by extracting these from the cement paste using warm water (50 °C) in accordance with the Japanese standard (Japan Industrial Standard, JIS A 1154 2012). Pulverized cement paste (10 g) and warm water (50 mL) were mixed for 30 min to extract the chloride ions. As previously mentioned, the mixture was separated, and the filtrate was potentiometrically titrated against silver nitrate using potentiometry.

3.5.3 Thermogravimetric Differential Thermal Analysis

The sample preparation was the same as that for the test above. The measurement of physically and chemically bound water was conducted under flowing N_2. The sample was heated at 10 °C/min from room temperature to 1000 °C using a thermogravimetric differential thermal analyzer (TG–DTA; Rigaku, TG 8120). Referring to previous studies (Saikia et al. 2006; Jalal et al. 2015), the bound water was quantified from the mass loss at 650 °C.

3.5.4 X-Ray Diffraction Analysis

The cement paste specimens were sealed and stored in a laboratory room (20 °C) for 28 days. Subsequently, the hardened specimens were crushed to 2.5–5.0 mm. The crushed particles were immersed in a 3% NaCl solution

for 28 days. To prevent hydration of the crushed cement paste, the test specimens were prepared by freeze-drying after immersion in acetone. The cement paste (90 mass%) was mixed with α-Al_2O_3 (10 mass%) and pulverized using a vibration mill. The addition of α-Al_2O_3 was employed for quantification of the observed phases (Friedel's salt and mono-carbonate). The XRD analysis was performed using a RIGAKU RINT 2500 V diffractometer. Table 4 lists the compounds identified and their diffraction peaks. The XRD measurement conditions are given in the footnote of Table 4. In addition, these hydrates were quantified by Rietveld analysis software "MDI JADE 6" using samples that had been immersed in 3% NaCl solution for 0 and 28 days (Shi et al. 2017). Moreover, in the XRD measurement, the compounds listed in Table 4 were identified by the Rietveld analysis.

4 Test Results and Discussion

4.1 Compressive Strength

Figure 2 shows the average compressive strengths of concrete made with ***w/cm*** of 0.55. The 7-day compressive strengths of concretes made with OPC and CG mixture (OPC-13%) were higher than those of other concretes. The admixture indicated a similar effect of silica fume reported in previous investigations (Bagheri et al. 2013; Madani et al. 2014). This result implied that the chloride ingress retarding admixture (CG) contributed to an increasing early-age strength of concrete. The 28-day compressive strengths of OPC incorporating SF or CG were almost equivalent and significantly higher than that of the control concrete (OPC, BB).

Figure 3 shows the relationships between the admixture (CG) content in concrete for each ***w/cm*** and their average 28-day compressive strengths. Regardless of ***w/cm***, the compressive strength was almost proportional to the increase in the admixture content. As mentioned in Table 1, the admixture has a BET specific surface area of 13,000 m^2/kg and contains significant Al_2O_3 and SiO_2. The superior strength properties of concrete made with the admixture (CG) are due to extensive ettringite formation and pozzolanic reactions, in addition to the micro-filler effect (Kasai and Sakai 2007). The ettringite formation temporarily contributes to increase of strength at an early age. The pozzolanic hydration and the micro-filler effect are dominant factors for the strength improvement.

Table 4 Hydration products.

Hydration product	Symbol	2θ
Ettringite ($C_3A{\cdot}3CaSO_4{\cdot}32H_2O$)	Et	9.1
Monosulfate ($C_3A{\cdot}CaSO_4{\cdot}12H_2O$)	Ms	9.9
Kuzel's salt ($C_3A{\cdot}0.5CaSO_4{\cdot}0.5CaCl_2{\cdot}10H_2O$)	KS	10.6
Friedel's salt ($C_3A{\cdot}CaCl_2{\cdot}12H_2O$)	FS	11.2
Monocarbonate ($C_3A{\cdot}CaCO_3{\cdot}11H_2O$)	Mc	11.6
Portlandite ($Ca(OH)_2$)	CH	18.0

Tube voltage: 30 kV; tube current: 100 mA; interval: 0.02°; time: 2 s/step; start–end positions: 5°–70° (for XRD measurement and Rietveld analysis).

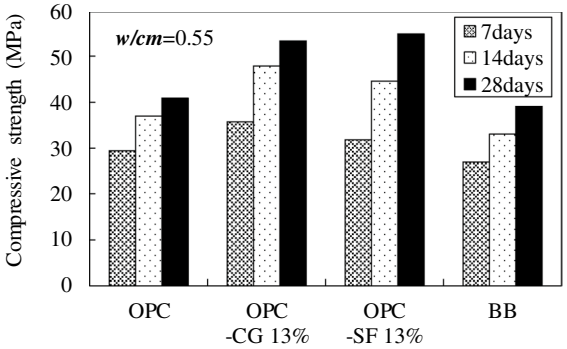

Fig. 2 Average compressive strength of each concrete composition.

4.2 Chloride Migration Test

Figure 4 shows the effective diffusion coefficients of chloride ions in the concretes. The results shown herein were obtained in the chloride migration test which used three specimens for each composition at the age of 28 days. The coefficient obtained for the OPC-CG13% concrete indicated the lowest value of those tested. According to similar studies (Ahmed et al. 2008; Farahani et al. 2015), OPC made with SF at a cement-replacement ratio of 10–13% will give a chloride ion diffusion coefficient that is significantly lower than that of BB concrete. It is notable that the OPC-CG13% concrete had a lower coefficient than that made with silica fume (OPC-SF13%).

Figure 5 shows that the effective chloride ion diffusion coefficients of concrete decreased with the increase

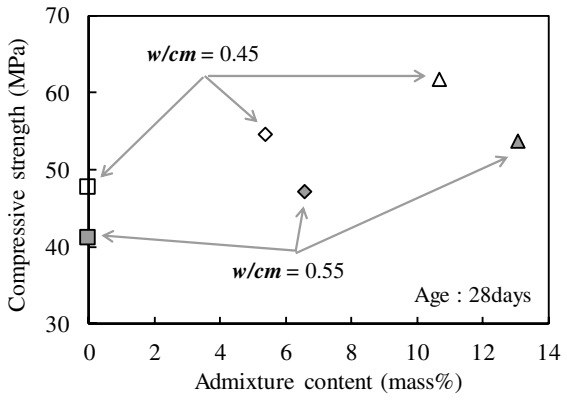

Fig. 3 Relation between admixture content and compressive strength.

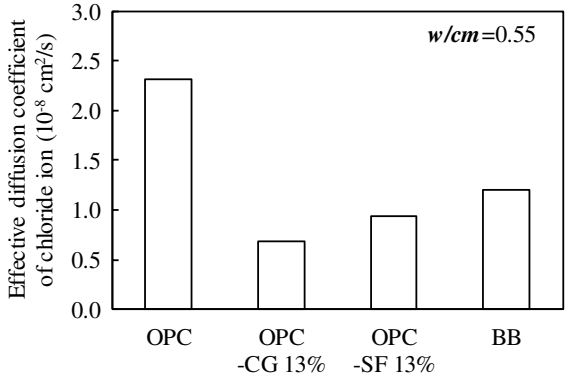

Fig. 4 Effective chloride diffusion coefficient of each concrete composition.

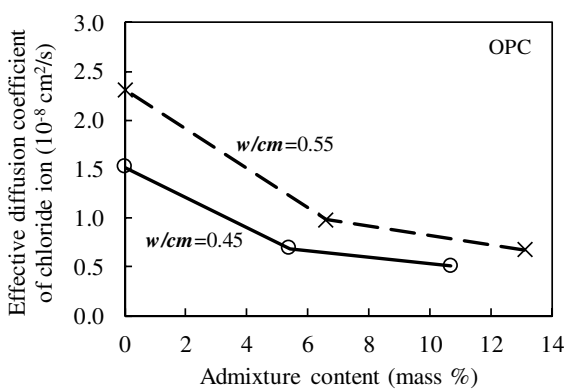

Fig. 5 Relation between admixture content and effective chloride diffusion coefficient.

of CG admixture content. This result confirmed that the coefficient can be decreased by adding the admixture as an alternative cementitious material in both ***w/cm*** concretes (***w/cm*** = 0.45, 0.55). Compared to the variation of the coefficient in the concrete of ***w/cm*** = 0.45, the significant decrease of the coefficient in the concrete of ***w/cm*** = 0.55 was noteworthy.

4.3 Chloride Immersion Test for Concrete

Cylindrical concrete specimens (OPC, OPC-CG7%, OPC-CG13%) were immersed for 91 days in a 10% NaCl solution. Figure 6 shows the apparent diffusion coefficients of chloride ions (D_{ap}) obtained for these concretes. The D_{ap} values were obtained from the average in three cylindrical specimens for each composition. The variability of these values was in the range of plus/minus 0.1×10^{-8} cm^2/s. The results confirm that the apparent diffusion coefficient of the concretes decreased in accordance with an increase in the amount of CG admixture.

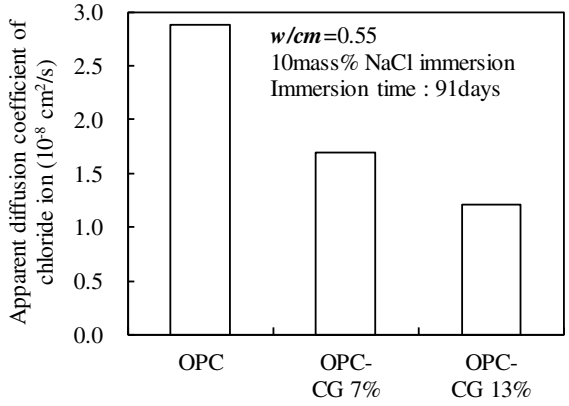

Fig. 6 Apparent chloride diffusion coefficient (D_{ap}).

4.4 Mechanism of Resistance Against Chloride Ingress

4.4.1 Densification Evaluated from Pore-Size Distribution

Figure 7 shows the pore-size distributions. The total pore volumes for each ***w/cm*** concrete (0.45, 0.55) were almost equivalent or gradually increased with increasing amount of admixture. The volume of pores having smaller diameter, especially fine pores having a diameter of 0.01 μm or lower, increased according to the amount of the admixture added. It is of interest that the increases of fine pore volume (lower 0.01 μm) were observed in both ***w/cm*** concretes. This observation confirmed that the admixture contributed to a denser pore structure of concrete by replacing the cement. It is notable that the concrete of ***w/cm*** = 0.55 contained a relatively higher volume of large pores while the fine pore volume of the concrete of ***w/cm*** = 0.55 was higher than the volume in concrete of ***w/cm*** = 0.45. In addition, the fine pore volume of OPC-CG13% (0.55) was slightly higher than the volumes of reference concretes, OPC-SF13% (0.55) and BB (0.55), which had almost an equivalent total pore volume. The denser structure is due to the microfiller effect and the pozzolanic reaction of the admixture (Hassana et al. 2012). Previous studies (Madani et al. 2014; Mehta and Monteiro 2006; Ando et al. 2015) reported that chloride-ion ingress slows down the increase of the fine pores volume. The high resistance to chloride-ion penetration mentioned previously was attributed to this change in pore-size distribution observed in this study.

4.4.2 Chemical Immobilization of Chloride Ion Evaluated from Change of Hydration Product

The chemical immobilization of chloride ions by the admixture was evaluated by investigating the amounts of chloride ions and the hydration products in cement paste immersed in 3% NaCl solution.

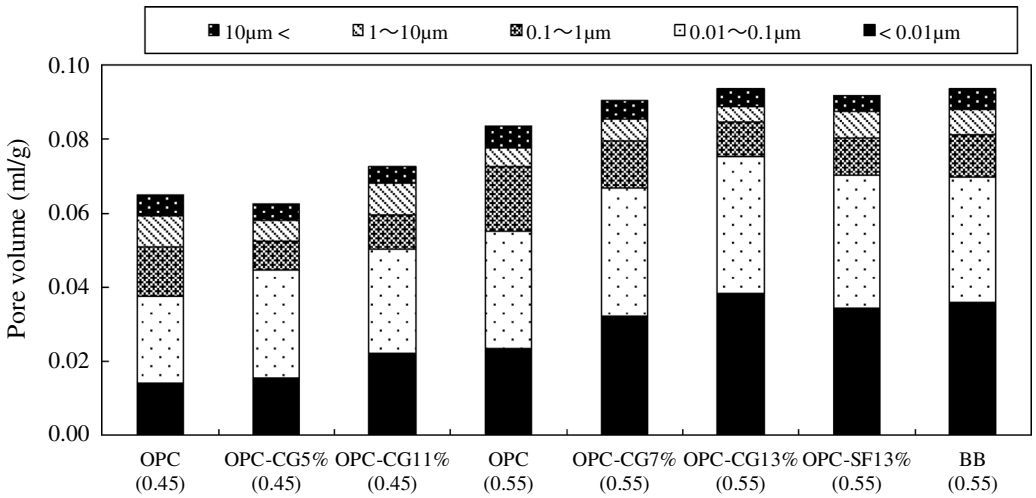

Fig. 7 Pore size distribution.

Figure 8a shows the total and bound amount of chloride-ions after immersion for 28 and 91 days. Both values increased with the increase in cement-replacement ratio of the admixture. There was slight difference between the results for 28 and 91 days of immersion. It should be noted that the binding capacity may vary over the depth of the specimen. These values shown herein were the average over the depth of the specimen and the local binding capacity was dependent on the local chloride content.

As well, Fig. 8b shows the decrease of the calcium hydroxide in accordance with the increase of the admixture content. The variation implies that Friedel's salt is increased by increasing the products of mono-carbonate, C–A–H and C–A–S–H. That is, the result indicates that the amount of the bound chloride ion can be increased by the increase in cement-replacement ratio of the admixture. In addition, the result confirmed the above-mentioned observation from the almost equivalent calcium hydroxide ($Ca(OH)_2$) contents after 28 and 91 days of immersion.

Figure 9 shows the changes of bound water contents in cement paste as a function of admixture content, respectively. As shown in Fig. 9, regardless of the cement-replacement ratio of the admixture, the amounts of bound water in both samples before immersion were similar at approximately 20%. The amount of bound water in cement paste immersed in a 3% NaCl solution increased till 28 days of immersion but remained almost constant until 91 days. This observation may indicate

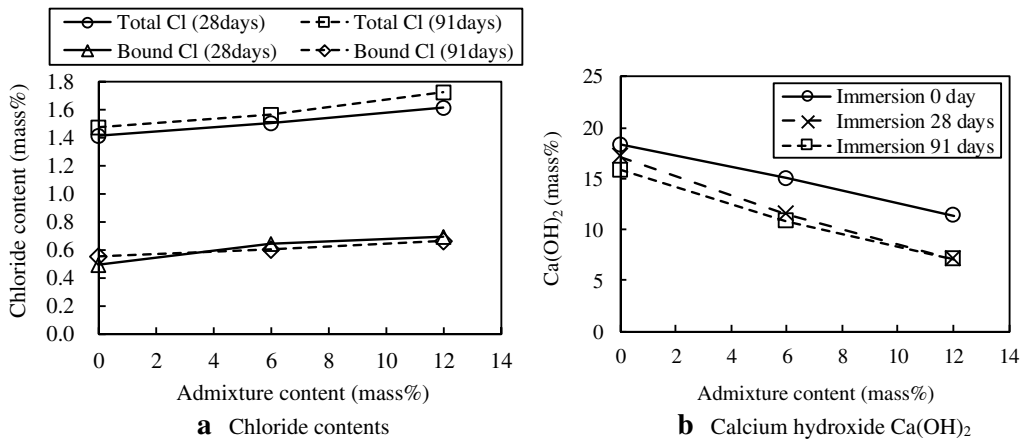

Fig. 8 Chloride and calcium hydroxide contents varied by the admixture content: (**a**) chloride contents; (**b**) calcium hydroxide $Ca(OH)_2$.

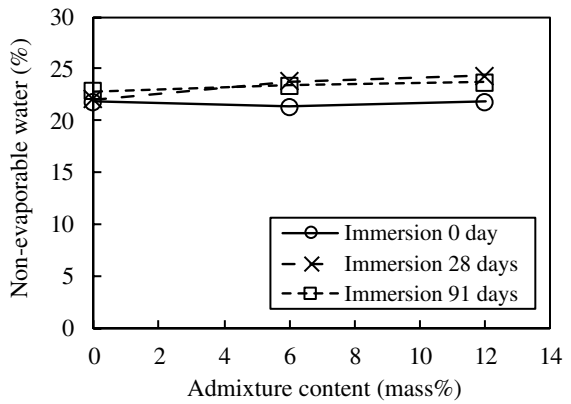

Fig. 9 Relation between admixture content and non-evaporable water.

that the degree of hydration of both the admixture and the cement hardly changes after the age of 28 days. This tendency corresponds with the results shown in Fig. 8, in which the bound chloride-ion amounts showed little difference between 28 and 91 days of immersion.

Changes in the hydration products were examined to confirm the function of the immobilizing chloride ions in the cement paste incorporating the admixture. Figure 10 shows the XRD charts of the cement-paste sample before and after 28 days of immersion in a 3% NaCl solution. The peak of the mono-carbonate was observed in the pattern of the pre-immersion cement paste (Celik et al. 2015). The admixture contains significant Al_2O_3, so the amount of aluminate hydrate was possibly increased by increasing the cement-replacement ratio of the admixture. Aluminium hydrate, however, hardly increased although the admixture reacted. Amorphous phases, such as C–A–H or C–A–S–H, which cannot be observed by XRD, were possibly generated. After immersion for 28 days, the mono-carbonate peak disappeared, and the peak attributed to Friedel's salt was observed. It is well known that Friedel's salt ($C_3A{\cdot}CaCl_2{\cdot}12H_2O$) fixes chloride by replacing CO_3^{2-} contained in monocarbonate ($C_3A{\cdot}CaCO_3{\cdot}11H_2O$) or SO_4^{2-} contained in monosulfate ($C_3A{\cdot}CaSO_4{\cdot}12H_2O$) with Cl^- (Shi et al. 2017; Glass et al. 1997). Rietveld analysis was performed to obtain a quantitative evaluation. The result showed that the content of Friedel's salt produced in 28 days of immersion was 4.6–7.6%, whereas the mono-carbonate content before immersion was 8.4–10.8%. Based on these observations, it was concluded that most of the mono-carbonate reacted with chloride ions to form Friedel's salt and the amount of chemically bound chloride ion was increased by the incorporation of the admixture. It should be noted that chemical bound effect may be gradually decreased due to the concrete carbonation. Further investigations are necessary to confirm the effect for long-term practical applications.

Figure 11 shows the relationship between the amounts of bound chloride ions and Al_2O_3 contained in the binder (OPC + CG). The amounts of chemically bound chloride ions were increased by the Al_2O_3. This result demonstrated that Al_2O_3 contributes to the binding of chloride by mechanisms such as the formation of Friedel's salt (Glass et al. 1997). Therefore, it was confirmed that densification of the hardened cement by the fine admixture and binding of chloride ions by formation of Friedel's salt both contributed to the increased resistance against chloride ingress.

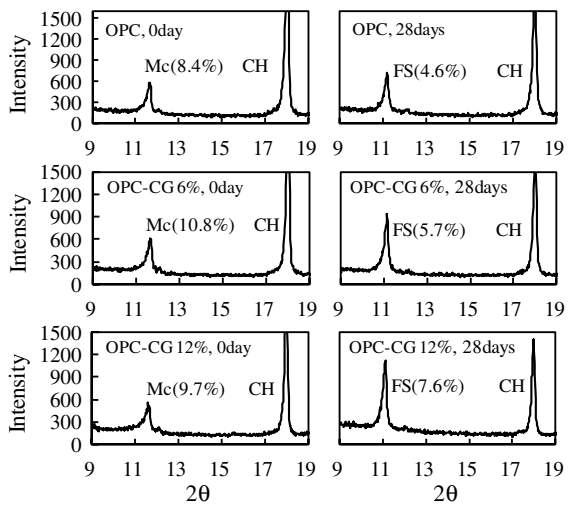

Fig. 10 XRD chart of cement paste.

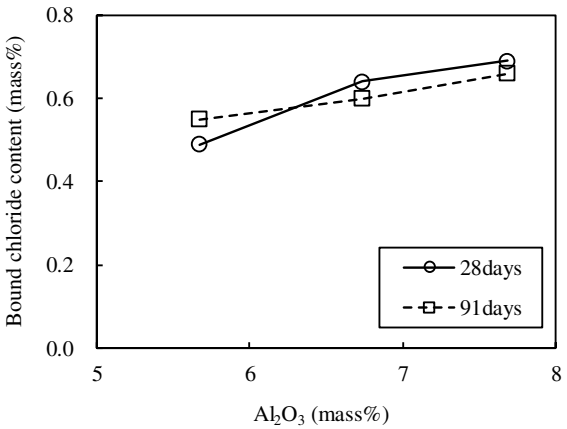

Fig. 11 Relation between Al_2O_3 content and chloride content.

5 Conclusions

This study investigated the chloride-penetration resistance and the mechanism thereof in concrete incorporating a developed pozzolanic admixture. The research addressed the properties of concrete cured under standard conditions to examine the applicability of the admixture to general ready-mix concrete. The conclusions of the experimental investigation are summarized as follows:

1. Concrete incorporating the developed admixture as a partial replacement of cement demonstrated a decrease in both the effective and apparent chloride diffusion coefficients. The chloride-penetration resistance of concrete with the admixture was superior to that of concrete incorporating silica fume at a similar cement-replacement ratio.
2. The compressive strength of the concrete with the developed admixture at 7 days age was higher than that of other tested concretes, such as OPC, OPC with 13% silica fume, and BB.
3. The volume of pores of smaller diameter increased with the increase of the admixture content, especially fine pores of 0.01 μm or smaller diameter increased. It was confirmed that the admixture contributes to creating a denser pore structure of concrete by replacing the cement.
4. Most of the mono-carbonate reacted with chloride ions to form Friedel's salt and the amount of bound chloride ions increased with the addition of the admixture.
5. It was confirmed that densification of the hardened cement matrix and bound of chloride ions by the formation of Friedel's salt improved the resistance against chloride ingress of concrete made with the admixture.

Acknowledgements
The authors thank Kathryn Sole, PhD, from Edanz Group (www.edanzediting.com/ac) for English language editing a draft of this manuscript. Also, we would like to thank Editage (www.editage.com) for editing of the revised manuscript.

Authors' contributions
KY designed the study, performed the experiments and wrote the manuscript. AS and TI conducted the experiments and analyzed the data. IY reviewed and edited the manuscript. All authors read and approved the final manuscript.

Funding
The authors gratefully acknowledge the financial support of Ube Industries.

Availability of data and materials
All data generated or analyzed during this study are included in this published article. The detailed data of the admixture are not publicly available due to the Japanese patent.

Competing interests
The authors declare that they have no competing interests.

Author details
[1] Cement and Construction Materials Company, Ube Industries, Ube, Japan. [2] Department of Civil and Environmental Engineering, Yamaguchi University, 2-16-1 Tokiwadai, Ube, Yamaguchi 755-8611, Japan.

Received: 24 April 2019 Accepted: 7 January 2020
Published online: 24 February 2020

References

Ahmed, M. S., Kayali, O., & Anderson, W. (2008). Chloride penetration in binary and ternary blended cement concretes as measured by two different rapid methods. *Cement & Concrete Composites, 30*(7), 576–582.
Amoudi, O. S. B., Kutti, W. A., Ahmad, S., & Maslehuddin, M. (2009). Correlation between compressive strength and certain durability indices of plain and blended cement concretes. *Cement & Concrete Composites, 31,* 672–676.
Ando, M., Kobayashi, H., Uenaka, S., & Nawa, T. (2015). Quantification of tortuosity of pore network for diffusion of chloride ion transport into hardened cement paste. *Cement Science and Concrete Technology, 69,* 96–103. **(in Japanese)**.
ASTM International. (2004a). ASTM C 494, Standard specification for chemical admixtures for concrete.
ASTM International. (2004b). ASTM C 1556, standard test method for determining the apparent chloride diffusion coefficient of cementitious mixtures by bulk diffusion.
Bagheri, A., Zanganeh, H., Alizadeh, H., Shakerinia, M., & Marian, M. A. S. (2013). Comparing the performance of fine fly ash and silica fume in enhancing the properties of concretes containing fly ash. *Construction and Building Materials, 47,* 1402–1408.
Celik, K., Jackson, M. D., Mancio, M., Meral, C., Emwas, A. H., Mehta, P. K., et al. (2014). High-volume natural volcanic pozzolan and limestone powder as partial replacements for portland cement in self-compacting and sustainable concrete. *Cement & Concrete Composites, 45,* 136–147.
Celik, K., Meral, C., Gursel, A. P., Mehta, P. K., Horvath, A., & Monteiro, P. J. M. (2015). Mechanical properties, durability, and life-cycle assessment of self-consolidating concrete mixtures made with blended portland cements containing fly ash and limestone powder. *Cement & Concrete Composites, 56,* 59–72.
Crank, J. (1975). *The mathematics of diffusion* (2nd ed.). Oxford: Oxford University Press.
Elrahman, M. A., & Hillemeier, B. (2014). Combined effect of fine fly ash and packing density on the properties of high performance concrete: An experimental approach. *Construction and Building Materials, 58,* 225–233.
European standards. (2011). EN 197-1, cement—Part 1: Composition, specifications and conformity criteria for common cements.
Fan, Y., Zhang, S., Kawashima, S., & Shah, S. P. (2014). Influence of kaolinite clay on the chloride diffusion property of cement-based materials. *Cement & Concrete Composites, 45,* 117–124.
Farahani, A., Taghaddos, H., & Shekarchi, M. (2015). Prediction of long-term chloride diffusion in silica fume concrete in a marine environment. *Cement & Concrete Composites, 59,* 10–17.
Glass, G. K., Hassanein, N. M., & Buenfeld, N. R. (1997). Neural network modeling of chloride binding. *Magazine of Concrete Research, 49*(181), 323–335.
Hassana, A. A. A., Lachemib, M., & Hossain, K. M. A. (2012). Effect of metakaolin and silica fume on the durability of self-consolidating concrete. *Cement & Concrete Composites, 34,* 801–807.
Heisig, A., Urbonas, L., Beddoe, R. E., & Heinz, D. (2016). Ingress of NaCl in concrete with alkali reactive aggregate: Effect on silicon solubility. *Materials and Structures, 49,* 4291–4303.
Hisada, M., Nagataki, S., & Otsuki, N. (1999). Evaluation of mineral admixtures on the viewpoint of chloride ion migration through mortar. *Cement & Concrete Composites, 21,* 443–448.
Hossain, M. M., Karim, M. R., Hasan, M., Hossain, M. K., & Zain, M. F. M. (2016). Durability of mortar and concrete made up of pozzolans as a partial replacement of cement: A review. *Construction and Building Materials, 116,* 128–140.

Ishida, T., Miyahara, S., & Maruya, T. (2007). Cl binding capacity of mortars made with various Portland cement and admixtures. *Doboku Gakkai Ronbunshuu E, 63*(1), 14–26. **(in Japanese)**.
Ishida, T., Yamato, K., Yamaji, N., & Tsugo, S. (2015). Physical properties of concrete using admixture for chloride attack. *Proceedings of the Japan Concrete Institute, 37*(1), 733–738. **(in Japanese)**.
Jalal, M., Pouladkhan, A., Harandi, O. F., & Jafari, D. (2015). Comparative study on effects of Class F fly ash, nano silica and silica fume on properties of high performance self-compacting concrete. *Construction and Building Materials, 94,* 90–104.
Japan Industrial Standard. (2006). JIS A 1108, method of test for compressive strength of concrete **(in Japanese)**.
Japan Industrial Standard. (2009a). JIS R 5210, portland cement **(in Japanese)**.
Japan Industrial Standard. (2009b). JIS R 5211, portland blast-furnace slag cement **(in Japanese)**.
Japan Industrial Standard. (2011a). JIS A 6204, chemical admixtures for concrete **(in Japanese)**.
Japan Industrial Standard. (2011b). JIS A 6207, silica fume for use in concrete **(in Japanese)**.
Japan Industrial Standard. (2012). JIS A 1154, methods of test for chloride ion content in hardened concrete **(in Japanese)**.
Japan Society of Civil Engineers. (2013). Standard specifications for concrete structures (test methods and specifications) **(in Japanese)**.
Juenger, M., & Siddique, R. (2015). Recent advances in understanding the role of supplementary cementitious materials in concrete. *Cement and Concrete Research, 78,* 71–80.
Kasai, Y., & Sakai, E. (2007). Admixture for concrete, Gijyutu-Shoin, pp. 61–76 **(in Japanese)**.
Lia, Q., Gengb, H., Huangd, Y., & Shuia, Z. (2015). Chloride resistance of concrete with metakaolin addition and seawater mixing: A comparative study. *Construction and Building Materials, 101,* 184–192.
Madani, H., Bagheri, A., Parhizkar, T., & Raisghasemi, A. (2014). Chloride penetration and electrical resistivity of concretes containing nanosilica hydrosols with different specific surface areas. *Cement & Concrete Composites, 53,* 18–24.
Meddah, M. S., Lmbachiya, M. C., & Dhir, R. K. (2014). Potential use of binary and composite limestone cements in concrete production. *Construction and Building Materials, 58,* 193–205.
Mehta, P. K., & Monteiro, P. J. M. (2006). *Concrete microstructure properties and materials* (4th ed., pp. 292–295). New York: McGraw Hill Education.
Ministry of Land, Infrastructure and Transport. (2015). Annual Report on the Japanese infrastructure and transport, pp. 122–124 **(in Japanese)**.
Neville, A. M. (2012). *Properties of concrete* (5th ed., pp. 565–577). London: Pearson Education Ltd.
Raupach, M. (2015). Chloride-induced macrocell corrosion of steel in concrete—theoretical background and practical consequences. *Construction and Building Materials, 101,* 184–192.
Sabet, F. A., Libre, N. A., & Shekarchi, M. (2013). Mechanical and durability properties of self-consolidating high performance concrete incorporating natural zeolite, silica fume and fly ash. *Construction and Building Materials, 44,* 175–184.
Saikia, N., Kato, S., & Kojima, T. (2006). Thermogravimetric investigation on the chloride binding behaviour of MK–lime paste. *Thermochimica, 444,* 16–25.
Schepper, M. D., Snellings, R., Buysser, K. D., Driessche, I. V., & de Belie, N. D. (2014). The hydration of cement regenerated from completely recyclable concrete. *Construction and Building Materials, 60,* 33–41.
Shi, Z., Geiker, M. R., Lothenbach, B., de Weerdt, K. D., Garzón, S. F., Rasmussen, K. E., et al. (2017). Friedel's salt profiles from thermogravimetric analysis and thermodynamic modelling of Portland cement-based mortars exposed to sodium chloride solution. *Cement & Concrete Composites, 78,* 73–83.
The International Organization for Standardization. (2005). ISO 1920-4, testing of concrete—Part 4—strength of hardened concrete.
Vaysburd, A. M., & Emmons, P. H. (2004). Corrosion inhibitors and other protective systems in concrete repair: Concepts or misconcepts. *Cement & Concrete Composites, 26,* 255–263.
Wattanachai, P., Otsuki, N., Saito, T., & Nishida, T. (2009). A study on chloride ion diffusivity of porous aggregate concretes and improvement method. *Doboku Gakkai Ronbunshuu E, 65*(1), 30–44.
Yamato, K., Ishida, T., Yamaji, N., Tsugo, S., & Yoshitake, I. (2017). Durability of steam-cured concrete incorporating a high-resistance admixture for chloride attack. *Journal of the Society of Materials Science Japan, 66*(5), 328–333. **(in Japanese)**.
Yoshida, N., Sakai, E., Mashimo, M., & Daimon, M. (2002). Fixation of chloride ion by the various type of cement in the marine environment. *Cement Science and Concrete Technology, 56,* 400–405. **(in Japanese)**.

Publisher's Note